Research Square

Preprints are preliminary reports that have not undergone peer review.
They should not be considered conclusive, used to inform clinical practice,
or referenced by the media as validated information.

Regulation Mechanism of Graphene Oxide on the Structure and Mechanical Properties of Bio-Based Gel-Spun Lignin/Poly (Vinyl Alcohol) Fibers

Yanhong Jin
Donghua University - Songjiang Campus: Donghua University
Yuanyuan Jing
Donghua University - Songjiang Campus: Donghua University
Wenxin Hu
Donghua University - Songjiang Campus: Donghua University
Jiaxian Lin
Donghua University - Songjiang Campus: Donghua University
Yu Cheng
Donghua University - Songjiang Campus: Donghua University
Xiaona Yang
Donghua University - Songjiang Campus: Donghua University
Kun Zhang
Donghua University - Songjiang Campus: Donghua University
Chunhong Lu (chlu@dhu.edu.cn)
Donghua University - Songjiang Campus: Donghua University https://orcid.org/0000-0003-4497-191X

Research Article

Keywords:

Posted Date: February 12th, 2021

DOI: https://doi.org/10.21203/rs.3.rs-184442/v1

License: This work is licensed under a Creative Commons Attribution 4.0 International License.
Read Full License

Version of Record: A version of this preprint was published at Cellulose on April 7th, 2021. See the published version at https://doi.org/10.1007/s10570-021-03859-x.

Regulation mechanism of graphene oxide on the structure and mechanical properties of bio-based gel-spun lignin/poly (vinyl alcohol) fibers

Yanhong Jin, Yuanyuan Jing, Wenxin Hu, Jiaxian Lin, Yu Cheng, Xiaona Yang, Kun Zhang, Chunhong Lu*

Key Laboratory of Textile Science & Technology, Ministry of Education, College of Textiles, Donghua University, Shanghai 201620, China

*Correspondence author's email: chlu@dhu.edu.cn

Abstract Lignin has been used as a sustainable and eco-friendly filler in composite fibers. However, lignin aggregation occurred at high lignin content, which significantly hindered the further enhancement of fiber performance. The incorporation of graphene oxide (GO) enhanced the mechanical properties of the lignin/poly(vinyl alcohol) (PVA) fibers and affected their structure. With the GO content increasing from 0 to 0.2%, the tensile strength of 5% lignin/PVA fibers increased from 491 MPa to 631 MPa, and Young's modulus increased from 5.91 GPa to 6.61 GPa. GO reinforced 30% lignin/PVA fibers also showed the same trend. The tensile strength increased from 455 MPa to 553 MPa, and Young's modulus increased from 5.39 GPa to 7 GPa. The best mechanical performance was observed in PVA fibers containing 5% lignin and 0.2% GO, which had an average tensile strength of 631 MPa and a Young's modulus of 6.61 GPa. The toughness values of these fibers are between 9.9-15.6 J/g, and the fibrillar and ductile fracture microstructure were observed. Structure analysis of fibers showed that GO

reinforced 5% lignin/PVA fibers had higher crystallinity, and evidence of hydrogen bonding among GO, lignin, and PVA in the gel fibers was revealed. Further, water resistance and swelling behavior of composite PVA fibers were studied to further evidence the structure change of composite fibers.

Graphic abstract

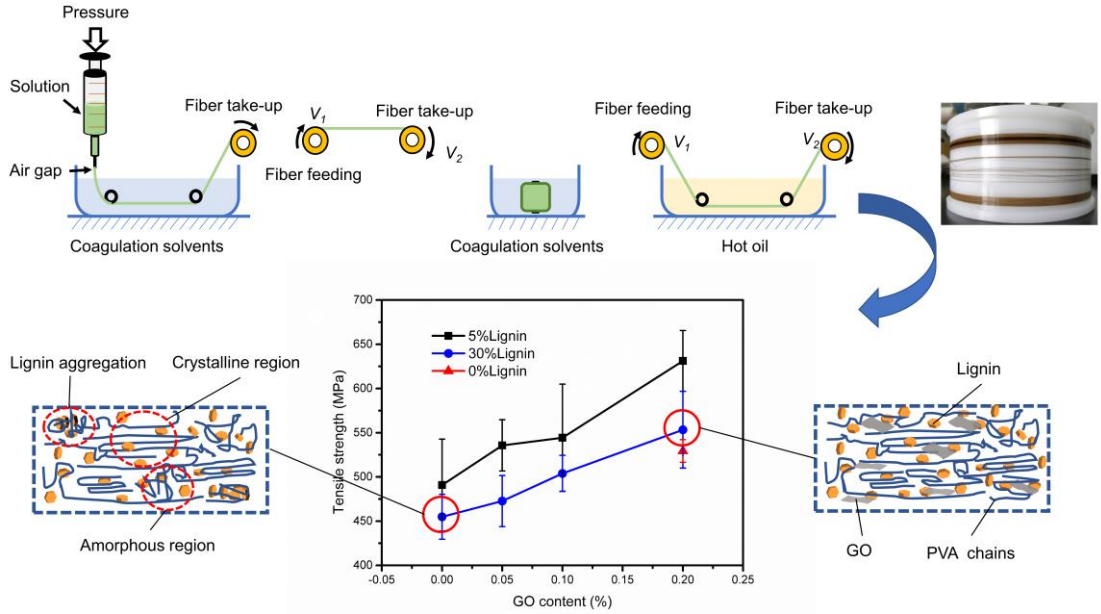

Keywords Gel spinning, Lignin, Graphene oxide, Poly (vinyl alcohol), Fibers, Reinforcement, Mechanism

Introduction

Poly(vinyl alcohol) (PVA) is a biopolymer with high hydrophilicity and good mechanical properties (Lu and Ford 2018), which is widely used as raw material for packaging film, textile sizing, and hydrogel (Iwaseya et al. 2005; Luo et al. 2018), etc. Similar to polyethylene (PE), the planar zigzag structure of PVA favors fiber-formation and makes it an ideal material for high-performance fibers (Kaufmann and Hesselbarth 2007; Sun et al. 2001). Fiber spinning techniques of PVA (i.e. wet spinning, dry spinning, melt spinning, and gel spinning, etc.) have been well developed in the past few decades (Cha et al. 1994). It is worth mentioning that gel spinning effectively reduces molecular chain entanglement during the spinning process, further promotes the fiber alignment in the drawing process, making it an efficient fabrication method

for high-performance PVA fibers (Smith and Lemstra 1980). Moreover, filler (i.e. lignin, carbon nanotubes, cellulose whiskers, etc.) reinforcement has been investigated as a promising way for further improvement of fiber properties (Lu et al. 2017a; Uddin et al. 2011; Xu et al. 2010).

Lignin, as the second most abundant biopolymer on earth, is present in all fibrous plants. Nearly 50 million tons of lignin are produced each year as a byproduct of pulp and paper-making industry, while only 2% is utilized commercially (Laurichesse and Avérous 2014). Due to its high char yield of ~50% (Thakur et al. 2014), lignin has been proposed as a cost-effective and renewable feedstock for carbon fibers (Baker and Rials 2013). However, compared to conventional polyacrylonitrile (PAN)-based carbon fibers, lignin-based carbon fibers have relatively lower mechanical properties (tensile strength of 400-700 MPa, Young's modulus of 40-95 GPa) (Kubo and Kadla 2005; Liu et al. 2015; Sudo and Shimizu 1992). Nevertheless, lignin has the potential to be used as an eco-friendly and sustainable filler in polymer due to its rigid structure. Lignin/PVA fibers have been spun by gel spinning (Lu et al. 2017a; Lu et al. 2017b). With the incorporation of 5% lignin, PVA fiber exhibited a tensile strength of 1.1 GPa and a Young's modulus of 36 GPa. Even at up to 50% lignin, lignin/PVA fibers had better mechanical properties than that of neat PVA fibers spun under optimum conditions (Lu et al. 2017a). As hydrogen bonding occurred between lignin and PVA hydroxyl groups, the molecular mobility of PVA enhanced, and fiber draw ratios increased. However, at lignin content of more than 20%, filler aggregation and poor alignment of lignin along the fiber axis were observed, which impeded the fabrication of even stronger lignin

reinforced PVA fibers (Lu et al. 2017a). To ultimately achieve high-performance lignin-based fibers, the intermolecular compatibility between lignin and PVA, as well as the molecular alignment in fiber structure should be further optimized.

Graphene is a two-dimensional carbon material with exceptional inherent mechanical properties, including extremely high tensile strength of 125 GPa and Young's modulus of 1000 GPa (Lee et al. 2008; Zhu et al. 2010). However, the weak interfacial interaction between the graphene nanofillers and the polymer matrix hinders the preparation of a homogeneous dispersion and further fibers with excellent mechanical performance. Graphene oxide (GO), with oxygen-containing groups (i.e. hydroxyl, carbonyl, carboxyl, and glycidyl groups) on the surface of nanosheets, has attracted considerable attention as filler for polymeric composites (Rourke et al. 2011; Wilson et al. 2009) due to its low cost, good mechanical performance and excellent compatibility with polymers (Liang et al. 2009). For instance, GO/PVA nanocomposite hydrogels with aligned hierarchical microstructure and anisotropic mechanical properties had been reported (Luo et al. 2018). Gel-spun GO/PVA nanocomposite fibers with GO nanosheets highly oriented along the fiber axis were also prepared (Hu et al. 2017). The tensile strength increased 46.15% after only 0.5 wt% GO nanosheets were incorporated into fibers. Although Hu et al. prepared GO/lignin/PVA films, the tensile strength of 100−125 MPa is far below the standards of industrial high-performance applications (Hu et al. 2019). Therefore, insufficient studies employ GO as filler in lignin/PVA gel-spun fibers to overcome the structural impediments of lignin/PVA fibers at high lignin contents for further enhancement in fiber performance or investigate the

synergistic effects of GO and lignin on the mechanical properties and structure of PVA fibers.

To better address the regulation mechanism of GO on the structure and mechanical properties of bio-based gel-spun lignin/PVA fibers, lignin/PVA, GO/PVA and GO/lignin/PVA composite fibers with varying lignin and GO contents utilizing gel-spinning technique were fabricated in this work. The prepared fibers were characterized structurally by scanning electron microscopy (SEM), X-ray diffraction analysis (XRD), and Fourier transform infrared spectroscopy (FTIR). Mechanical performance, water resistance, and swelling ratios were also evaluated, and the effects of lignin and GO on the fiber structure were discussed. This study will possibly expand the application of low-cost bio-based high-performance fibers in industry.

Experimental section

Materials

PVA (M_w=146,000−186,000, 99% hydrolysis, Sigma-Aldrich Co., USA) and graphene oxide aqueous dispersion (GO, concentration of 10 mg/mL, sheets diameter of 5-8 μm, Hangzhou Gaoxi Technology Co., Ltd., China) were used as received. Lignin (purity of 90%, Hubei Yunmei Technology Co., Ltd., China) was used after purification. Dimethyl sulfoxide (DMSO, Sigma-Aldrich Co., USA), acetone, and methanol (Shanghai Titan Technology, Inc., China) were used as received. All water used was deionized.

Preparation of spinning dopes

To remove low-molecular-weight fractions, lignin was first dissolved in acetone and then purified by vacuum filtration. Later, it was washed by deionized (DI) water for multiple times and dried in a vacuum oven at 65 °C for 4 h. Finally, lignin was ground into fine powder by the mortar and pestle.

Three types of solution mixtures (GO/PVA, lignin/PVA, and GO/lignin/PVA) were prepared for spinning. To prepare GO/PVA solution, GO (at weight ratios of 0.2% (w/w) GO to polymer) and PVA powder (10 g) were dissolved in 100 mL of 80/20 (v/v) DMSO/DI water under constant stirring at 85 °C for 2 h. For the lignin/PVA solutions, PVA powder (10 g) and lignin, at weight ratios of 5% and 30% (w/w) lignin to polymer, were dissolved in 100 mL of 80/20 (v/v) DMSO/DI water under constant stirring at 85 °C for 2 h, respectively. To prepare GO/lignin/PVA dopes, at weight ratios of 5% and 30% (w/w) lignin to polymer, concentrations of 0.05%, 0.1% and 0.2% (w/w) GO to polymer were also dissolved in 80/20 (v/v) DMSO/DI water at the same condition, respectively. All prepared solutions were maintained at 65 °C before spinning.

Gel spinning

The gel spinning process is illustrated in four steps (Fig. 1). Steps 1 involves the loading of polymer dope (50 mL) into a syringe maintained at 60 °C and the extrusion of the polymeric jet through a 0.72 mm inner diameter syringe needle. Lignin/PVA and GO/lignin/PVA polymeric jets were injected into acetone/methanol (85/15 v/v) coagulation solvents maintained at −25 °C with an air gap of 3-5mm due to that

methanol could facilitate PVA gel fiber formation but partially dissolve lignin while acetone could effectively hinder the lignin diffusion from fiber structure into coagulation solvents (Lu et al. 2017a). GO/PVA fibers were spun into 100% methanol coagulation solvent for good fiber formation under the same spinning condition. All as-spun fibers which underwent 1 m length coagulation bath were later collected onto a rotating take-up winder. The collected as-spun fibers were air drawn at room temperature (Step 2) before storage in coagulation solvents with the same compositions as the ones in Step 1 for gel aging at 5 °C for 24 h (Step 3). Step 4 involves the hot drawing of fibers through silicone oil bath for four stages at high temperature (100−220 °C). The draw ratio (*DR*) of each drawing stage was calculated by Equation (1):

$$DR=\frac{V_2}{V_1} \quad (1)$$

where V_1 represents the velocity of the fiber feeding winder and V_2 represents the velocity of the fiber take-up winder, respectively (Fig. 1, Step 2 & 4). Drawing parameters for gel-spun fibers are listed in Table 1, which will be discussed later.

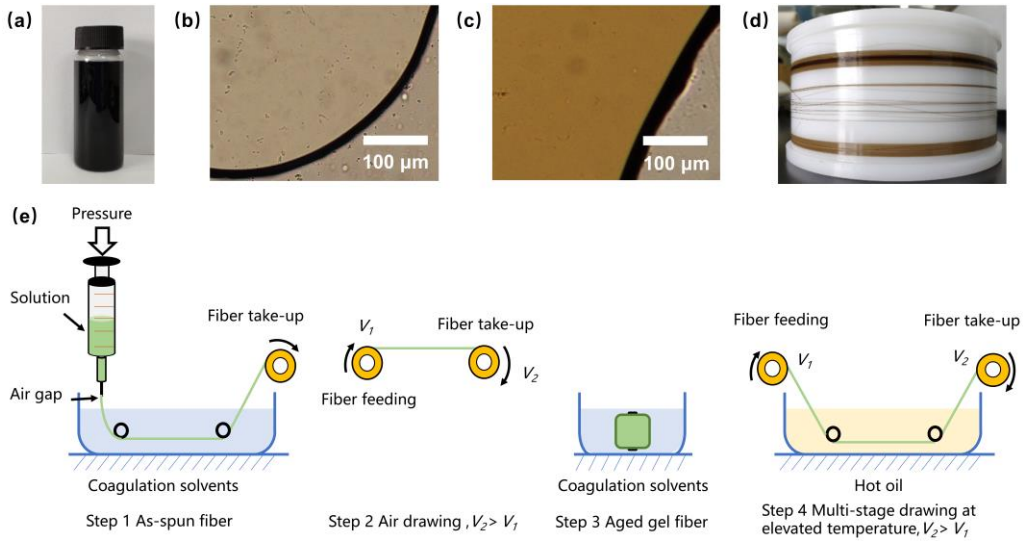

Fig. 1 Homogeneity of GO/lignin/PVA dopes: (a) digital photograph of 0.2% GO/30%

lignin/PVA solution, and optical micrographs of (b) 0.2% GO/5% lignin/PVA and (c) 0.2% GO/30% lignin/PVA spinning solutions; (d) digital photograph of 30% lignin/PVA drawn fibers prepared by gel spinning, (e) the fiber gel spinning process: as-spun gel fiber formation (Step 1), air drawing (Step 2), gel fiber aging (Step 3), and multiple-stage fiber drawing (Step 4)

Mechanical testing

The mechanical properties of fibers were measured with the XQ-1C tensile testing system according to ASTM D3379. Mechanical testing was performed with a 20 mm gauge length, a strain rate of 15 mm/min, and a sample size of 10. Values of fiber cross-sectional area A were determined gravimetrically from measurements of linear density, d, and the density of the composite fiber ρ, using Equation (2):

$$A = d/\rho \quad (2)$$

where d values were obtained by weighing the mass of 30 cm composite fibers. Before weighing, the fibers were rinsed by isopropyl alcohol to remove residual silicone oil on the fiber surface and dried at room temperature for 24 h. Values of ρ were calculated by Equation (3):

$$\rho = \rho_{PVA} w_{PVA} + \rho_{lignin} w_{lignin} + \rho_{GO} w_{GO} \quad (3)$$

where w is the weight fraction of PVA, lignin, and GO, respectively. The density of both PVA (Luo et al. 2013) and lignin (Hu 2002) is 1.3 g/cm^3, and the density of GO is 2.2 g/cm^3 (Hu et al. 2017). The weight fraction of GO (0.05%, 0.1%, or 0.2%) was so small that it could be negligible. Therefore, the density of each composite fiber was

approximately ρ = 1.3 g/cm^3.

Tensile toughness (U_t) was calculated from the integration of the stress-strain curve of each composite fiber. It represents the energy absorbed during the fiber breakage process (Song et al. 2013), which can be expressed by Equation (4):

$$U_t = \int \sigma_i \varepsilon_i \quad (4)$$

where σ_i and ε_i are the stress and strain at each data point *i*, respectively.

Imaging analysis

A SU8010 scanning electron microscopy was used to study the morphology of the fiber facture tips after mechanical testing. Fractured fiber samples were sputter coated with gold and imaged by SEM at 5 kV accelerating voltage.

Fiber structural analysis

X-ray Diffraction patterns of fibers were collected by Rigaku D/max-2550 PC X-ray Diffractometer using Cu K_α radiation (λ = 1.541 Å) at voltage of 40 kV and operating current of 150 mA. Shredded fibers were scanned at a step size of 0.05° with 2θ between 5° and 60°.

Peak fitting was performed by MDI Jade 6 software. The percent crystallinity (X_c) of each composite fiber was calculated based on crystalline (A_c) and amorphous (A_a) peak areas (Minus et al. 2006):

$$X_c\ (\%) = \left(\frac{A_c}{A_c + A_a}\right) \times 100\% \quad (5)$$

Aligned fiber bundles of more than 100 fibers with 3 cm in length were placed on

187 the sample holder and scanned for molecular anisotropy. Cu K_α radiation (λ = 1.541 Å)
188 at voltage of 40 kV and operating current of 150 mA were applied. Fibers were scanned
189 in the equator and meridian directions at a step size of 0.05° with 2θ between 5° and
190 60°. Then the detector was fixed at the 2θ position of the strongest peak, and the sample
191 holder rotated from -90° to 270° along the azimuth angle to test the intensity distribution
192 of the diffraction peak. Peak fitting was performed by MDI Jade 6 software. The
193 orientation (y) is calculated by Equation (6) (Zhu et al. 2009):

194 $$y\,(\%) = \frac{360\text{-}\sum H_i}{360} \times 100\% \quad (6)$$

195 where H_i is the half-height width at peak i.

196 The structural analysis of fibers was performed for 128 scans at 4 cm^{-1} spectral
197 resolution on the NEXUS-670 Fourier transform infrared spectrophotometer equipped
198 with attenuated total reflection.

199 FTIR spectra in the 800-4200 cm^{-1} range were normalized to the 854 cm^{-1} band
200 (C−C stretching) (Peppas 1977; Tretinnikov and Zagorskaya 2012). The C–C stretching
201 peak is chosen as a reference due to that its absorbance is not significantly affected by
202 processing. Percent crystallinity (X_c) of polymer is expressed in Equation (7):

203 $$X_c = \left(a + b\frac{A_{1114}}{A_{854}}\right) \times 100\% \quad (7)$$

204 where a=14.40 and b=24.09 are constants whose values are calculated from known
205 values of percent crystallinity from X-ray diffraction patterns (Fig. S1，S2 and Table
206 S1 in Supplementary Information, SI). Absorbance values for A_{1144} and A_{854} were
207 calculated from infrared spectra.
208

Water dissolution and swelling

To investigate the water resistance of PVA fibers with different lignin and GO contents, fiber bundles (2 mg) designated as (lignin to PVA)/(GO to PVA) ratios of 0/0.01, 0/0.02, 5/0, 5/0.05, 5/0.1, 5/0.2, 30/0, 30/0.05, 30/0.1, and 30/0.2, were placed in 25 mL of water and gradually heated from 25 to 85 °C. Optical images of fibers were obtained by optical microscope (ECLIPES LV100N POL) after water immersion of fibers. To study the swelling behavior of GO/lignin/PVA fibers, fiber bundles were immersed in DI water for 24 h at room temperature. Post immersion, the fibers were blotted with filter paper to remove excess water before being weighed. The fiber swelling ratio (S) was calculated according to Equation (8):

$$S=\frac{m_w-m_d}{m_d}\times 100\% \quad (8)$$

where m_d and m_w represent the mass of the fiber before and after wetting, respectively.

Results and discussion

Effect of GO on lignin/PVA fiber drawing process

In this section, the drawing parameters for all gel-spun composite fibers, including drawing ratios, drawing temperature, effective diameters, and linear density, were summarized in Table 1. Changes in drawing temperature and drawing ratios of each stage were observed.

As the first drawing process after the as-spun fibers being collected from the coagulation bath, air drawing facilitates the alignment of molecular chains, the

reduction of the fiber diameter, and promotes the solvent exchange in the subsequent gel aging process (Zhang et al. 2011). With the air drawing process applied, the subsequent thermal drawing of gel-spun fibers is more stable, which may contribute to the enhanced strength, toughness, and dimensional stability of the gel-spun fibers, which will be further evidenced in the later section.

Table 1. Drawing parameters for gel-spun lignin/PVA, GO/PVA, and GO/lignin/PVA fibers

Lignin content		0		5%			30%			
GO content		0.2%	0	0.05%	0.1%	0.2%	0	0.05%	0.1%	0.2%
As-spun	*DR*	1.9	1.8	1.9	1.8	1.8	1.8	1.7	1.8	2.1
Air drawing	*DR*	2.5	2.3	2.5	2.5	2	2.3	2	2.5	1.8
Stage 1	T/°C	105	110	120	105	105	125	115	110	110
drawing	*DR*	1.2	1.5	1.6	1.5	1.8	1.5	2.2	1.8	1.7
Stage 2	T/°C	180	180	180	180	180	180	190	180	180
drawing	*DR*	2	1.5	1.4	1.2	1.3	1.5	1.2	1.3	1.2
Stage 3	T/°C	200	200	205	200	200	200	200	200	200
drawing	*DR*	1.3	1.1	1.1	1.1	1.2	1.1	1.2	1.1	1.2
Stage 4	T/°C	225	220	220	220	220	215	215	220	220
drawing	*DR*	1.1	1.1	1.1	1.1	1.1	1.1	1.1	1.1	1.1
Total *DR*[a]		16.3	11.3	12.9	9.8	11.1	11.3	11.8	12.7	10.2
Effective diameter /μm		50	58	54	62	49	64	54	59	55
Linear density *d*/dtex		26	34	30	39	25	41	30	36	31

[a]Total *DR* is the cumulative draw ratio from as-spun drawing, air drawing, and hot drawing.

After gel aging of the air-drawn fibers in the coagulation solvents for 24 h, gel fibers were further drawn in hot oil for multiple stages at elevated temperatures. In the first stage, the drawing temperature of fibers is between 105−120 °C. It was observed that solvent diffused from the fibers into the high-temperature oil during the first stage of thermal drawing, which facilitate the conversion of gel fibers into solid fibers. The temperature was increased to 180-190 ℃ in the second stage of thermal drawing. There was still slight solvent diffusion during this stage, which was attributed to the residual DMSO (with a boiling point of 189 °C) in the fibers. In the third and fourth stages, the fibers were further drawn to obtain finer structure at increased drawing temperature. Effective diameters and linear density of fibers are shown in Table 1. Changes of GO/lignin/PVA fibers in stage drawing ratios were slight. The draw ratio of 0.2%GO/PVA fiber could reach 16.3, while the total draw ratios of GO/lignin/PVA fibers were in the range of 9.8-12.9 regardless of the content of lignin. It is possible that the intermolecular interaction in the GO/lignin/PVA ternary system, which will be shown in the later section, impeded the enhancement of fiber draw ratios.

Effect of GO content on lignin/PVA fiber mechanical properties

The effect of GO content on the tensile strength and Young's modulus of gel-spun lignin/PVA fibers is discussed in this section. Generally speaking, fibers with 5% lignin have significantly better mechanical properties than those with 30% lignin content, which is attributed to the higher crystallinity (as shown in Table 2), the stronger hydrogen bonding between lignin and PVA, and the better molecular orientation of 5%

lignin/PVA fiber (Lu et al. 2017a). After adding GO, fibers containing both GO and lignin fillers exhibited superior mechanical properties compared to those containing only lignin fillers (Fig. 2). As the GO content increased from 0 to 0.2%, the tensile strength of 5% lignin/PVA fibers increased from 491 MPa to 631 MPa, and Young's modulus increased from 5.91 GPa to 6.61 GPa. The 30% lignin/PVA fibers showed the same trend as the GO content increased from 0 to 0.2%: the tensile strength increased from 455 MPa to 553 MPa, and Young's modulus increased from 5.39 GPa to 7 GPa. The maximum tensile strength was 631 MPa at 0.2%GO/5% lignin, and the maximum modulus was 7 GPa at 0.2% GO/30% lignin.

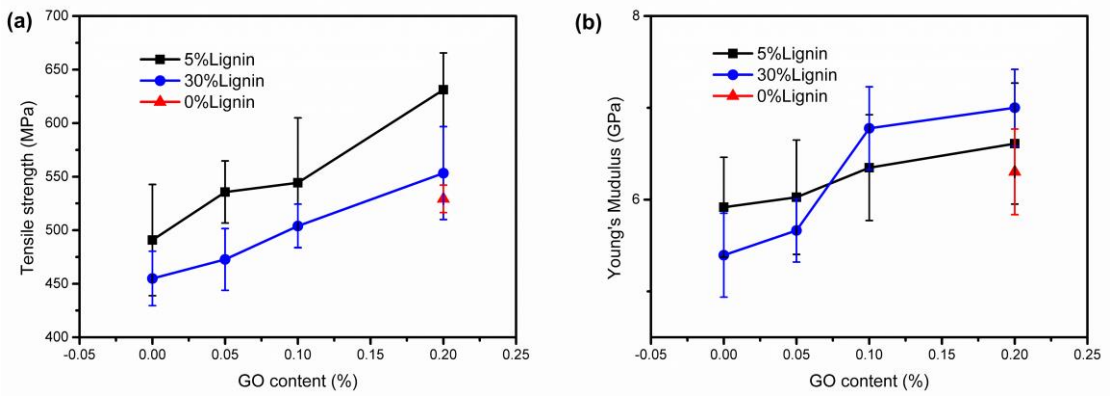

Fig. 2 Tensile strength and Young's modulus of gel-spun PVA fibers of 0/5/30% lignin and 0/0.05%/0.1%/0.2% GO

It was clearly shown that for GO/lignin/PVA composite fibers, both 5% and 30% lignin/PVA fibers had the best mechanical properties at 0.2% GO. To better verify the role of lignin in the ternary system of composite fibers, 0.2% GO/PVA fibers were fabricated and tested for comparison. Fig. 2 showed that the tensile strength (529 MPa) and Young's modulus (6.3 GPa) of 0.2% GO/PVA fiber were lower than those of 0.2%

GO/lignin/PVA fiber, confirming that lignin may work as an efficient filler in GO/PVA fibers and that the synergistic effect of GO, lignin and PVA results in the enhancement of fiber properties.

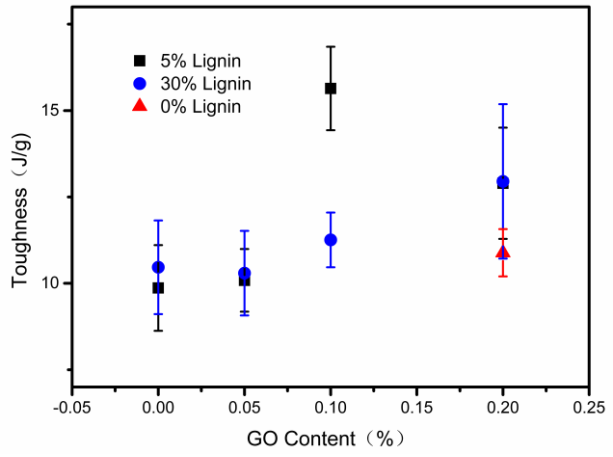

Fig. 3 Toughness of gel-spun PVA fibers with 0/5/30% lignin and 0/0.05%/0.1%/0.2% GO

The effect of GO content on gel-spun lignin/PVA fiber toughness is shown in Fig. 3. Toughness indicates fiber's ability to absorb mechanical energy before rupture (Shin et al. 2012). The strain at break values for all of the lignin/PVA and GO/lignin/PVA fibers ranged between 5.5% and 7.5% regardless of the filler content. Toughness values of GO/lignin/PVA fibers with varying GO and lignin contents ranged from 9.9 to 15.6 J/g, which were much greater than that of reported GO/PVA composites fiber (6 J/g)(Shin et al. 2012). A maximum toughness value of 15.6 J/g was observed in 0.1% GO/5% lignin/PVA fibers. As the GO content increased, the toughness of both 5% and 30% lignin/PVA fibers slightly increased. Compared with 0.2%GO/5% and 30%lignin/PVA composite fibers, 0.2%GO/PVA fiber had a lower toughness value (10.88 J/g). This indicates that lignin with a large amount of rigid structure can more

297 effectively increase the fiber toughness than GO.

298 Effect of GO content on lignin/PVA fiber structure

299 Fiber fracture tips from mechanical testing were imaged by SEM, as shown in Fig.
300 4. It was observed that all fibers had a dense structure without pores. Fiber diameters
301 were in the range of 50-65 μm, which were consistent with the effective diameters
302 calculated in Table 1. The fibrillar structure of the 0.2% GO/PVA fiber was also
303 observed (Fig. S3 in SI). The addition of GO could effectively enhance the strength of
304 the PVA fiber (Hu et al. 2017) and the fibrillar structure indicated the highly aligned
305 polymer chains along the fiber axis. 5% lignin/PVA fiber showed a smooth fracture tip
306 (Fig. 4a). With 0.2% GO incorporated, 0.2% GO/5% lignin/PVA fiber exhibited more
307 fibrillar microstructure and more ductile fracture tip (Fig. 4b). PVA fibrils are related to
308 the highly oriented and ordered polymer chains, which are responsible for the good
309 mechanical properties (tensile strength of 631 MPa, Young's modulus of 6.61 GPa).
310 The fibrillar structure was observed in 30% lignin/PVA fiber (Fig. 4c), which was
311 possibly due to the plasticizing effect of lignin (Lu et al. 2017a). The fibrillar structure
312 was also observed in 0.2% GO/30% lignin/PVA fiber (Fig. 4d). Even in high-resolution
313 images, no aggregation of lignin or GO was observed in the 0.2% GO/30% lignin/PVA
314 fiber, which only demonstrated uniform structure without obvious defects. In summary,
315 both lignin and GO promoted the formation of PVA fibrillar structure and were
316 responsible for the enhancement of mechanical properties aforementioned.

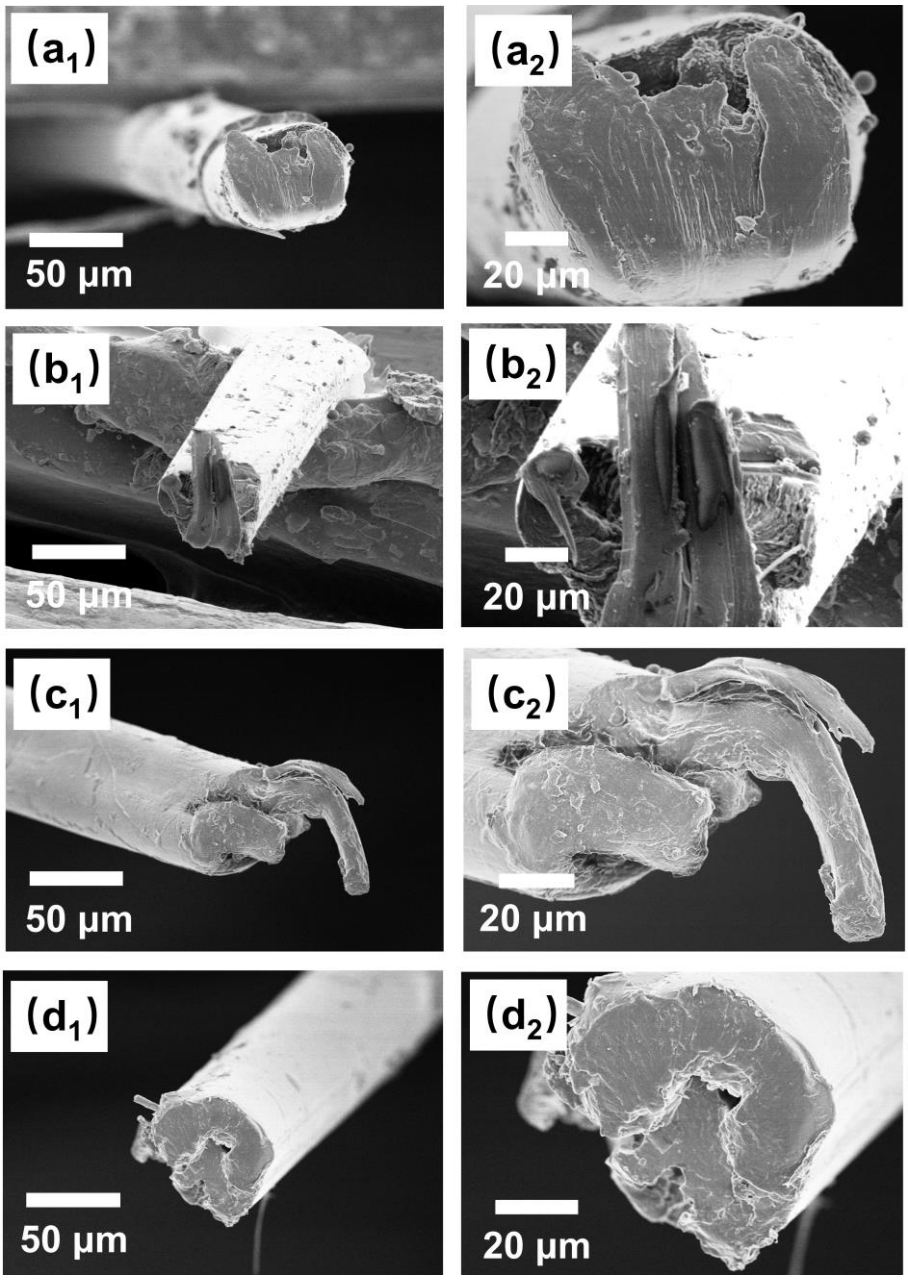

317

318 **Fig. 4** (1) Low- and (2) high-resolution SEM images of fracture tips of (a) 5% lignin

319 /PVA fibers, (b) 0.2% GO/5% lignin/PVA fibers, (c) 30% lignin/PVA fibers, (d) 0.2%

320 GO/30% lignin/PVA fibers

321

322 To better understand the effect of GO filler on the mechanical properties of

323 lignin/PVA fibers, fiber crystallinity, and molecular alignment will be discussed in this

324 section. Both molecular adhesion and orientation of polymer chains contribute to the

enhancement of mechanical performance of fibers (Gonzalez et al. 2014; Minus et al. 2009; Spitalsky et al. 2010). Thus both FTIR and XRD were used to indicate the structure change of gel-spun lignin/PVA fibers before/after the incorporation of GO.

FTIR spectra of PVA composite fibers in Fig. 5 together with XRD patterns (Fig. S1 in SI） were used to calculate the constants *a* and *b* in Equation (7) for further confirmation of all of the percent crystallinity of composite PVA fibers (Table 2). Amorphous PVA is related to the C-O vibrational mode at 1094 cm^{-1}, and PVA crystallinity affects the peak at 1144 cm^{-1} (Lu et al. 2017a). The value of the A_{1144}/A_{854} ratio is an index of fiber crystallinity. The crystallinity of PVA composite fibers (Table 2) approximately agreed with overall trends shown for the mechanical properties of fibers (Fig. 2). In detail, fibers with 5% lignin were more crystalline than those containing 30% lignin. Both 5% and 30% lignin fibers with GO showed higher or close crystallinity values in comparison with fibers without GO. This is due to that the presence of GO in the crystalline region promotes the formation of crystals, which will be demonstrated later in Fig. 6. The highest degree of crystallinity occurred at 0.05% GO/5% lignin, however, the value slightly decreased when GO content was more than 0.05% in 5% lignin/PVA fibers. Fibers with 30% lignin and 0.2% GO were obviously more crystalline than those containing 0/0.05% GO/0.1% GO, which had a similar value of crystallinity.

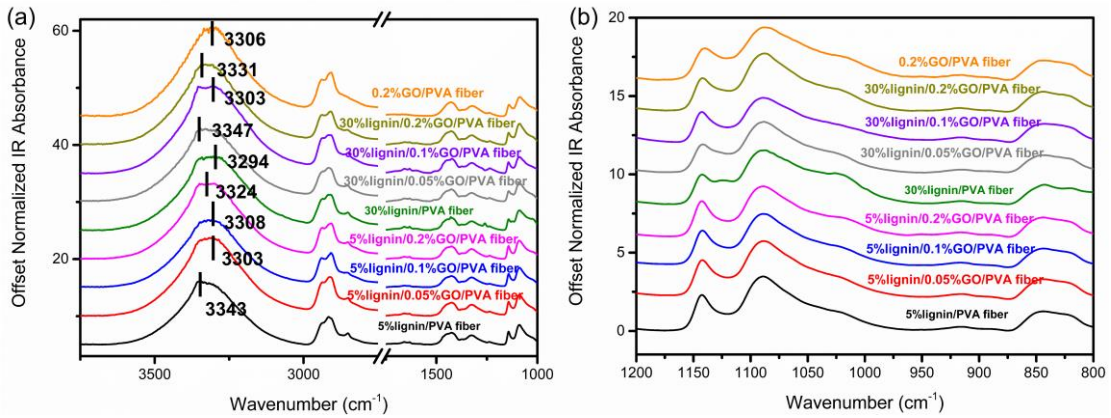

Fig. 5 FTIR absorbance spectra of gel-spun composite fibers between (a) 4200−1000 cm^{-1} and (b) 1250−800 cm^{-1}

Table 2 FTIR absorbance ratios of A_{1144}/A_{854} and percent crystallinity (X_c) of fibers with different lignin and GO contents

Sample	A_{1144}/A_{854}	X_c/%
0.2% GO/PVA	1.91	51.78
5% lignin/PVA	2.24	56.35
0.05% GO/5% lignin/PVA	2.44	59.70
0.1% GO/5%lignin/PVA	2.38	58.36
0.2% GO/5%lignin/PVA	2.29	56.40
30% lignin/PVA	1.98	52.60
0.05% GO/30% lignin/PVA	1.97	52.46
0.1% GO/30% lignin/PVA	1.99	52.75
0.2% GO/30% lignin/PVA	2.12	54.62

Moreover, FTIR spectra implied the molecular interaction among GO, lignin and PVA. The peaks at 2942 cm^{-1}, 1440 cm^{-1}, 1086 cm^{-1}, and 854 cm^{-1} were associated with the vibrations of C-H stretching, -CH_2 bending, C-O-C asymmetric stretching, and C-C stretching, respectively. It was obvious that in GO/PVA, lignin/PVA, and GO/lignin/PVA composite fibers, no new absorbance peaks occurred with the incorporation of lignin or GO, suggesting that no new functional groups were formed.

Intermolecular bonding among lignin, GO and PVA induces molecular adhesion. FTIR absorbance spectra from 3000 to 3700 cm^{-1} (Fig. 5a) provides insight into hydrogen bonding. The -OH stretching vibration peak of 5% lignin/PVA fiber is at 3343 cm^{-1}. With the addition of 0.05% GO, the peak shifted to lower frequencies, indicating shorter distances between oxygen atoms (O···O) from different hydroxyl groups (Jiang et al. 2012). The shift was possibly the result of intermolecular hydrogen bonding formed among GO, lignin, and PVA (Kubo and Kadla 2003). With higher GO content, the OH group absorbance peak shifted slightly to the higher frequencies, which might be due to the dissociation of hydrogen bonding between PVA molecular chains. The -OH stretching vibration peak of 30% lignin/PVA fiber was at 3294 cm^{-1}, indicating that the hydrogen bonding between PVA and lignin was strong. With the incorporation of GO, the peak shifted to higher frequencies at different levels, indicating that no more hydrogen bonding formed. Strong molecular interactions among composite fibers indicated good compatibility among GO, lignin, and PVA. As a result, gel-spun composite fibers showed no evidence of filler aggregation within the fiber microstructure (Fig. 4) and possessed good mechanical performance (Fig. 2).

In addition to the percent crystallinity investigation of fibers, XRD patterns (Fig. S4, SI) were also used to investigate the orientation of crystallites in polymers. As shown in Table 3, all fibers exhibited a high orientation of >90%. This verifies that gel-spinning technique is an effective method of fabricating fibers with high molecular orientation (Smith and Lemstra 1980). Taken both percent crystallinity and orientation into consideration, the former may be the main factor that differentiated the mechanical

performance of the fabricated fibers in this work since the molecular orientation of the polymer chains was similar.

Table 3 Orientation (y) of gel-spun composite fibers

Sample	y/%
0.2% GO/0% lignin/PVA	92.6
0% GO/5% lignin/PVA	91.8
0.1% GO/5% lignin/PVA	90.0
0.2% GO/5% lignin/PVA	92.0

The reinforcement mechanism of GO in lignin/PVA fibers

The microstructure models of spinning dopes and fibers are shown in Fig. 6 to better illustrate the structure of GO reinforced lignin/PVA fibers. The distribution of GO, lignin, and PVA in the homogenous spinning dope is random (Fig. 6a). Entanglements between the PVA macromolecular chains exist and hydrogen bonding can be formed among GO, lignin, and PVA since they all have oxygen-containing functional groups. After the gel-spun solid fiber is obtained, take 5% lignin/PVA fiber as an example, both crystalline and amorphous regions exist in the fiber structure (Fig. 6b$_1$). PVA molecular chains are highly aligned along the fiber axis and partially crystallized, which are indicated by percent crystallinity and orientation results in Tables 2 and 3**.** Intramolecular bonding of PVA can be replaced by intermolecular interaction between lignin and PVA, which reduces the entanglement between macromolecules and is beneficial to the formation of crystalline regions. However, when the lignin increased to 30%, the amorphous structure of excessive filler results in the decrease of fiber crystallinity. In addition, the aggregation (Fig. 6b$_2$) of lignin may

hinder the alignment of the PVA chains and cause a further decrease of the crystallinity. With the incorporation of a small amount of GO, hydrogen bonding is formed between GO/lignin, GO/PVA in addition to lignin/PVA. More crystalline areas are formed in GO reinforced lignin/PVA fibers in comparison with that of 5% and 30% lignin/PVA fibers (Fig. 6c$_1$ and 6c$_2$). No lignin aggregation was observed in the SEM images of GO reinforced 30% lignin/PVA fiber (Fig. 4d), indicating that hydrogen bonding between GO/lignin, GO/PVA promotes the even distribution of lignin in the fiber structure and the formation of crystals. However, due to the plasticizing effect and amorphous structure of lignin, the crystallinity of GO reinforced 30% lignin/PVA fiber is lower than that of GO reinforced 5% lignin/PVA fiber (Table 2).

In summary, the enhancement of GO reinforced lignin/PVA fiber properties could be attributed to the following three reasons. First, GO has excellent inherent mechanical properties (tensile strength of 125 GPa and Young's modulus of 1000 GPa) (McAllister et al. 2007). When the composite fiber is under tension, the load is effectively transferred from the polymer matrix to GO, the mechanical properties of the fiber are therefore improved. Secondly, GO has good compatibility with PVA and lignin. Hydrogen bonding can be formed among them, which effectively avoids the aggregation of excessive lignin and the formation of fiber structure defects. Finally, the addition of GO favors the alignment of PVA molecular chains along the fiber axis, which is beneficial to the formation of crystalline regions (Table 2).

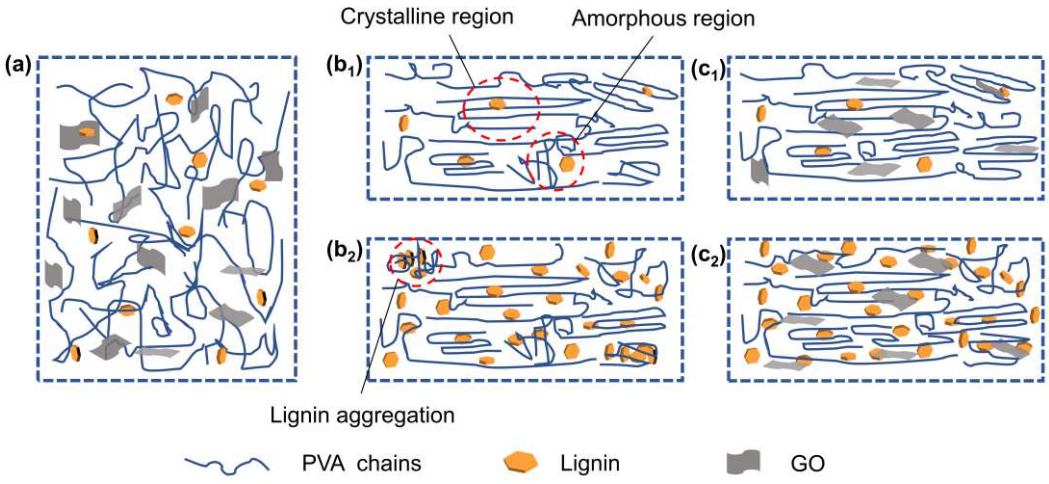

419

420 **Fig. 6.** The microstructure model of (a) GO/lignin/PVA spinning dope and (1) 5% (2)

421 30% lignin/PVA fibers (b) without and (c) with GO

422 Water resistance of composite fibers

423 PVA fibers are susceptible to water at elevated temperatures due to their polar

424 chemical structure (Lu et al. 2017a). In this study, it was evidenced that lignin and GO

425 could promote the water resistance behavior of composite PVA fibers since swelling

426 behavior was observed at elevated temperatures.

427

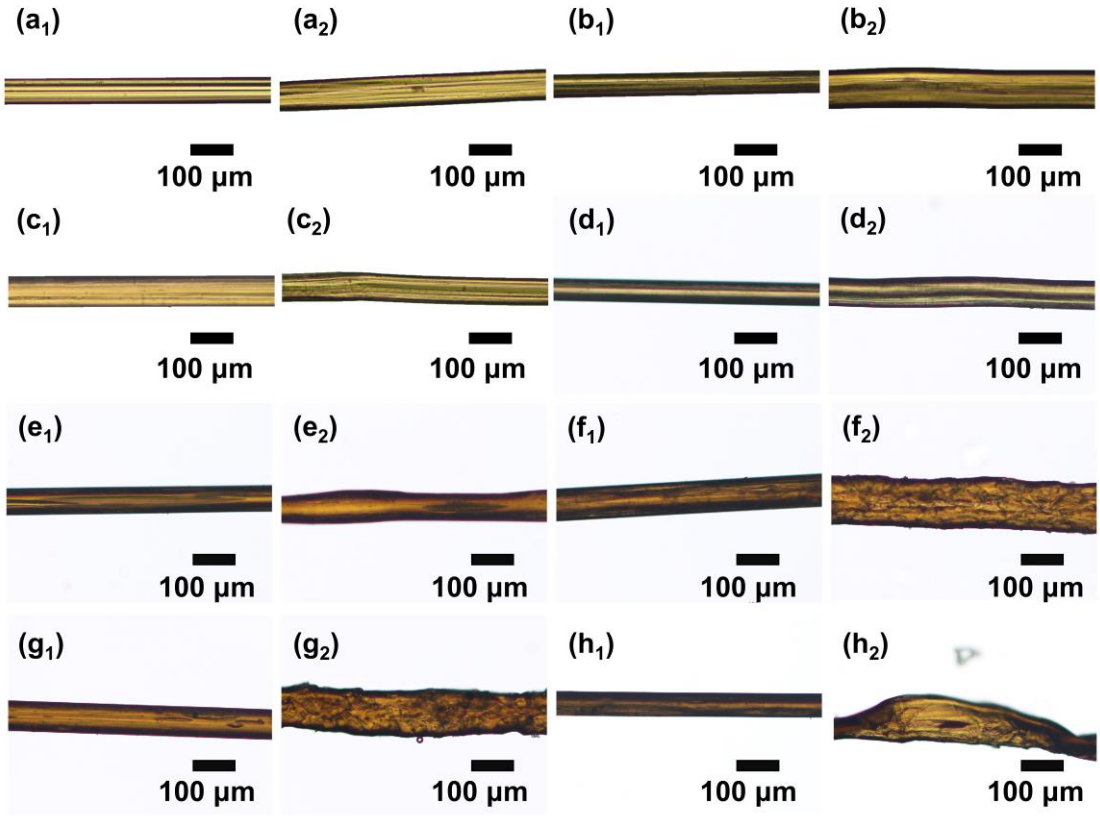

Fig. 7 Optical micrographs of (a) 5% lignin/PVA fiber, (b) 0.05% GO/5% lignin/PVA fiber, (c) 0.1% GO/5% lignin/PVA fiber, (d) 0.2% GO/5% lignin/PVA fiber, (e) 30% lignin/PVA fiber, (f) 0.05% GO/30% lignin/PVA fiber, (g) 0.1% GO/30% lignin/PVA fiber, (h) 0.2% GO/30% lignin/PVA fiber after water immersion at (1) 25 °C and (2) 85 °C

The dissolution of GO/PVA, lignin/PVA, and GO/lignin/PVA composite fibers were tested in water at different temperatures. Water resistance behavior of the composite fibers at room temperature and high temperature was observed by an optical microscope (Fig. 7). After being immersed in water at 25°C, all fibers showed intact structures. Although pure PVA fibers are soluble in water at 85 ℃ (Lu et al. 2017a), the dissolution of PVA fibers in water at 85 ℃ is hindered with the incorporation of lignin

441 or GO due to the intermolecular hydrogen bonding among GO, lignin, and PVA. In
442 detail, 0.2% GO/PVA fiber had an increase in diameter due to swelling in hot water at
443 85 °C, and it still maintained its intact fiber structure (Fig. S5, SI). At 5% lignin, the
444 GO/lignin/PVA fibers (Fig. 7a_2-d_2) exhibited increased diameter by swelling in water at
445 85 ℃. At 30% lignin (Fig. 7 e_2-h_2), the GO/lignin/PVA fibers immersed in water at 85 ℃
446 showed more significant swelling behavior and gel-like structure under the optical
447 microscope. The possible explanation could be that PVA fibers with 30% lignin content
448 had more amorphous region (lower crystallinity) than that of 5% lignin/PVA fibers, thus
449 the amorphous region in PVA fibers absorbed more water. Moreover, with GO content
450 increased from 0 to 0.2%, both 5% and 30% lignin/PVA fibers exhibited more obvious
451 swollen structure, which was possibly attributed to that the hydrogen bonding formation
452 of GO/lignin, GO/PVA and lignin/PVA promotes the structural network formation in
453 the swollen fibers.

454 To further study the structural difference between fully drawn composite fibers,
455 swelling ratio (*S*) revealing moisture uptake capability of fibers at room temperature
456 was measured and presented in Table 4. GO content had no significant influence on the
457 moisture uptake of fibers with 5% lignin and 30% lignin. At the same GO content (i.e.
458 0.2%), when lignin content increased from 0% to 30%, the swelling ratio increased
459 slightly from 5.13% to 6.67%. This was due to that PVA fibers with 30% lignin were
460 less crystalline so that the amorphous regions absorbed more water than PVA fibers
461 with 0% and 5% lignin. The most crystalline 0.05% GO/5% lignin /PVA fiber exhibited
462 a swelling ratio of 4.09%, which was lower than other fibers. These results agree with

463 the structural analysis of percent crystallinity shown in Table 2.

464

465 **Table 4** Swelling ratios (*S*) of gel-spun fibers after 24 h of water immersion.

Fiber	*S* (%)	Fiber	*S* (%)
0.2% GO/0% lignin/PVA	5.13	/	/
0% GO/5% lignin/PVA	5.69	0% GO/30% lignin/PVA	6.45
0.05% GO/5% lignin/PVA	4.09	0.05% GO/30% lignin/PVA	7.06
0.1% GO/5% lignin/PVA	4.76	0.1% GO/30% lignin/PVA	6.84
0.2% GO/5% lignin/PVA	5.26	0.2% GO/30% lignin/PVA	6.67

466 **Conclusions**

467 We have successfully fabricated gel-spun bio-based GO/lignin/PVA fibers which
468 demonstrate promising results of mechanical performance. With the incorporation of
469 GO, the aggregation of fillers was avoided and enhancement in fiber mechanical
470 properties was observed. With the GO content increasing from 0 to 0.2%, the tensile
471 strength of 5% lignin/PVA fiber increased from 491 MPa to 631 MPa, and Young's
472 modulus increased from 5.91 GPa to 6.61 GPa. GO reinforced 30% lignin/PVA fibers
473 also exhibited the same increasing trend. The tensile strength increased from 455 MPa
474 to 553 MPa, and Young's modulus increased from 5.39 GPa to 7 GPa. Thus, GO favors
475 the formation of defect-free fiber structure and the enhancement of fiber performance.
476 The structural enhancement at 0.2% GO/5% lignin/PVA fiber was evidenced by its high
477 crystallinity, intermolecular bonding among lignin, GO, and PVA, and good alignment
478 of molecular chains. The good mechanical performance of gel-spun GO/lignin/PVA
479 fibers indicates their potential for use in industrial and high-performance applications.

480

Acknowledgments

The authors are deeply grateful for the financial support received from the National Natural Science Foundation of China (Grant no. 51903033), Shanghai Sailing Program, China (Grant no. 19YF1400800), and Fundamental Research Funds for the Central Universities (Grant nos. 20D110110 and 2232020G-01).

Author information

Affiliation:

Key Laboratory of Textile Science & Technology, Ministry of Education, College of Textiles, Donghua University, Shanghai 201620, China

*Correspondence author's email: chlu@dhu.edu.cn

Compliance with ethical standards

Conflict of interest The authors declare that they have no conflict of interest.

References

Baker DA, Rials TG (2013) Recent advances in low-cost carbon fiber manufacture from lignin. Journal of Applied Polymer Science 130:713-728 doi:10.1002/app.39273

Cha WI, Hyon SH, Ikada Y (1994) Gel spinning of poly(vinyl alcohol) from dimethyl sulfoxide/water mixture. Journal of Polymer Science Part B-Polymer Physics 32:297-304 doi:10.1002/polb.1994.090320211

503 Gonzalez JS, Luduena LN, Ponce A, Alvarez VA (2014) Poly(vinyl alcohol)/cellulose
504 nanowhiskers nanocomposite hydrogels for potential wound dressings. Materials Science
505 & Engineering C-Materials for Biological Applications 34:54-61
506 doi:10.1016/j.msec.2013.10.006
507 Hu M, Chen Z, Luo S, Yang X, Ye R, Zheng M, Chen P (2019) Preparation of graphene oxide
508 and alkali lignin nanohybrids and its application to reinforcing polymer. Wood Science
509 and Technology 53:649-664 doi:10.1007/s00226-019-01094-z
510 Hu TQ (2002) Chemical modification, properties, and usage of lignin. Springer, New York
511 Hu X et al. (2017) Highly aligned graphene oxide/poly(vinyl alcohol) nanocomposite fibers
512 with high-strength, antiultraviolet and antibacterial properties. Composites Part A: Applied
513 Science and Manufacturing 102:297-304 doi:10.1016/j.compositesa.2017.08.015
514 Iwaseya M, Watanabe M, Yamaura K, Dai LX, Noguchi H (2005) High performance films
515 obtained from PVA/Na_2SO_4/H_2O and PVA/CH_3COONa/H_2O systems. Journal of Materials
516 Science 40:5695-5698 doi:10.1007/s10853-005-1429-6
517 Jiang X, Tan B, Zhang X, Ye D, Dai H, Zhang X (2012) Studies on the properties of poly(vinyl
518 alcohol) film plasticized by urea/ethanolamine mixture. Journal of Applied Polymer
519 Science 125:697-703 doi:10.1002/app.34957
520 Kaufmann J, Hesselbarth D (2007) High performance composites in spun-cast elements.
521 Cement & Concrete Composites 29:713-722 doi:10.1016/j.cemconcomp.2007.06.001
522 Kubo S, Kadla JF (2003) The formation of strong intermolecular interactions in immiscible
523 blends of poly(vinyl alcohol) (PVA) and lignin. Biomacromolecules 4:561-567
524 doi:10.1021/bm025727p

525 Kubo S, Kadla JF (2005) Lignin-based carbon fibers: effect of synthetic polymer blending on
526 fiber properties. Journal of Polymers and the Environment 13:97-105 doi:10.1007/s10924-
527 005-2941-0
528 Laurichesse S, Avérous L (2014) Chemical modification of lignins: towards biobased polymers.
529 Progress in Polymer Science 39:1266-1290 doi:10.1016/j.progpolymsci.2013.11.004
530 Lee C, Wei X, Kysar JW, Hone J (2008) Measurement of the elastic properties and intrinsic
531 strength of monolayer graphene. Science 321:385-388 doi:10.1126/science.1157996
532 Liang J, Huang Y, Zhang L, Wang Y, Ma Y, Guo T, Chen Y (2009) Molecular-Level Dispersion
533 of Graphene into Poly(vinyl alcohol) and Effective Reinforcement of their
534 Nanocomposites. Advanced Functional Materials 19:2297-2302
535 doi:10.1002/adfm.200801776
536 Liu HC, Chien A-T, Newcomb BA, Liu Y, Kumar S (2015) Processing, structure, and properties
537 of lignin- and CNT-incorporated polyacrylonitrile-based carbon fibers. ACS Sustainable
538 Chemistry & Engineering 3:1943-1954 doi:10.1021/acssuschemeng.5b00562
539 Lu C, Blackwell C, Ren Q, Ford E (2017a) Effect of the coagulation bath on the structure and
540 mechanical properties of gel-spun lignin/poly(vinyl alcohol) fibers. ACS Sustainable
541 Chemistry & Engineering 5:2949-2959 doi:10.1021/acssuschemeng.6b02423
542 Lu C, Ford E (2018) Antiplasticizing behaviors of glucarate and lignin bio-based derivatives on
543 the properties of gel-spun poly(vinyl alcohol) fibers. Macromolecular Materials and
544 Engineering 303 doi:10.1002/mame.201700523
545 Lu C, Rawat P, Louder N, Ford E (2017b) Properties and structural anisotropy of gel-spun
546 lignin/poly(vinyl alcohol) fibers due to gel aging. ACS Sustainable Chemistry &

547 Engineering 6:679-689 doi:10.1021/acssuschemeng.7b03028
548 Luo J, Li Q, Zhao T, Gao S, Sun S (2013) Bonding and toughness properties of PVA fibre
549 reinforced aqueous epoxy resin cement repair mortar. Construction and Building Materials
550 49:766-771 doi:10.1016/j.conbuildmat.2013.08.052
551 Luo Q, Shan Y, Zuo X, Liu J (2018) Anisotropic tough poly(vinyl alcohol)/graphene oxide
552 nanocomposite hydrogels for potential biomedical applications. RSC Advances 8:13284-
553 13291 doi:10.1039/c8ra00340h
554 McAllister MJ et al. (2007) Single sheet functionalized graphene by oxidation and thermal
555 expansion of graphite. Chemistry of Materials 19:4396-4404 doi:10.1021/cm0630800
556 Minus ML, Chae HG, Kumar S (2006) Single wall carbon nanotube templated oriented
557 crystallization of poly(vinyl alcohol). Polymer 47:3705-3710
558 doi:10.1016/j.polymer.2006.03.076
559 Minus ML, Chae HG, Kumar S (2009) Interfacial crystallization in gel-spun poly(vinyl
560 alcohol)/single-wall carbon nanotube composite fibers. Macromolecular Chemistry and
561 Physics 210:1799-1808 doi:10.1002/macp.200900223
562 Peppas NA (1977) Infrared spectroscopy of semicrystalline poly(vinyl alcohol) networks.
563 Macromolecular Chemistry and Physics 178:596-601
564 Rourke JP, Pandey PA, Moore JJ, Bates M, Kinloch IA, Young RJ, Wilson NR (2011) The real
565 graphene oxide revealed: stripping the oxidative debris from the graphene-like sheets.
566 Angew Chem Int Ed Engl 50:3173-3177 doi:10.1002/anie.201007520
567 Shin MK et al. (2012) Synergistic toughening of composite fibres by self-alignment of reduced
568 graphene oxide and carbon nanotubes. Nature Communications 3:650

569 doi:10.1038/ncomms1661
570 Smith P, Lemstra PJ (1980) Ultra-high-strength polyethylene filaments by solution
571 spinning/drawing. Journal of Materials Science 15:505-514
572 Song P, Xu Z, Guo Q (2013) Bioinspired strategy to reinforce PVA with improved toughness
573 and thermal properties via hydrogen-bond self-assembly. ACS Macro Letters 2:1100-1104
574 doi:10.1021/mz4005265
575 Spitalsky Z, Tasis D, Papagelis K, Galiotis C (2010) Carbon nanotube–polymer composites:
576 Chemistry, processing, mechanical and electrical properties. Progress in Polymer Science
577 35:357-401 doi:10.1016/j.progpolymsci.2009.09.003
578 Sudo K, Shimizu K (1992) A new carbon fiber from lignin. Journal of Applied Polymer Science
579 44:127-134
580 Sun W, Chen HS, Luo X, Qian HP (2001) The effect of hybrid fibers and expansive agent on
581 the shrinkage and permeability of high-performance concrete. Cement and Concrete
582 Research 31:595-601 doi:10.1016/s0008-8846(00)00479-8
583 Thakur VK, Thakur MK, Raghavan P, Kessler MR (2014) Progress in green polymer
584 composites from lignin for multifunctional applications: a review. ACS Sustainable
585 Chemistry & Engineering 2:1072-1092 doi:10.1021/sc500087z
586 Tretinnikov ON, Zagorskaya SA (2012) Determination of the degree of crystallinity of
587 poly(vinyl alcohol) by FTIR spectroscopy. Journal of Applied Spectroscopy 79:521-526
588 Uddin AJ, Araki J, Gotoh Y (2011) Toward "strong" green nanocomposites: polyvinyl alcohol
589 reinforced with extremely oriented cellulose whiskers. Biomacromolecules 12:617-624
590 doi:10.1021/bm101280f

591 Wilson NR et al. (2009) Graphene oxide: structural analysis and application as a highly
592 transparent support for electron microscopy. ACS Nano 3:2547-2556
593 Xu X, Uddin AJ, Aoki K, Gotoh Y, Saito T, Yumura M (2010) Fabrication of high strength
594 PVA/SWCNT composite fibers by gel spinning. Carbon 48:1977-1984
595 doi:10.1016/j.carbon.2010.02.004
596 Zhang W, Zhu Y, Zhu X, Zhang J, Huang X, Fu J (2011) Study on high strength PVA fiber
597 produced by DMSO method. Synthetic Technology and Application 26:7-11
598 Zhu Y, Cao Q, Chen X, Zha L (2009) Crystallite orientation and spiral structure of cotton:part
599 Ⅰ. Journal of Donghua University (Natural Science) 35:626-631
600 Zhu Y, Murali S, Cai W, Li X, Suk JW, Potts JR, Ruoff RS (2010) Graphene and graphene oxide:
601 synthesis, properties, and applications. Advanced Materials 22:3906-3924
602 doi:10.1002/adma.201001068
603

Figures

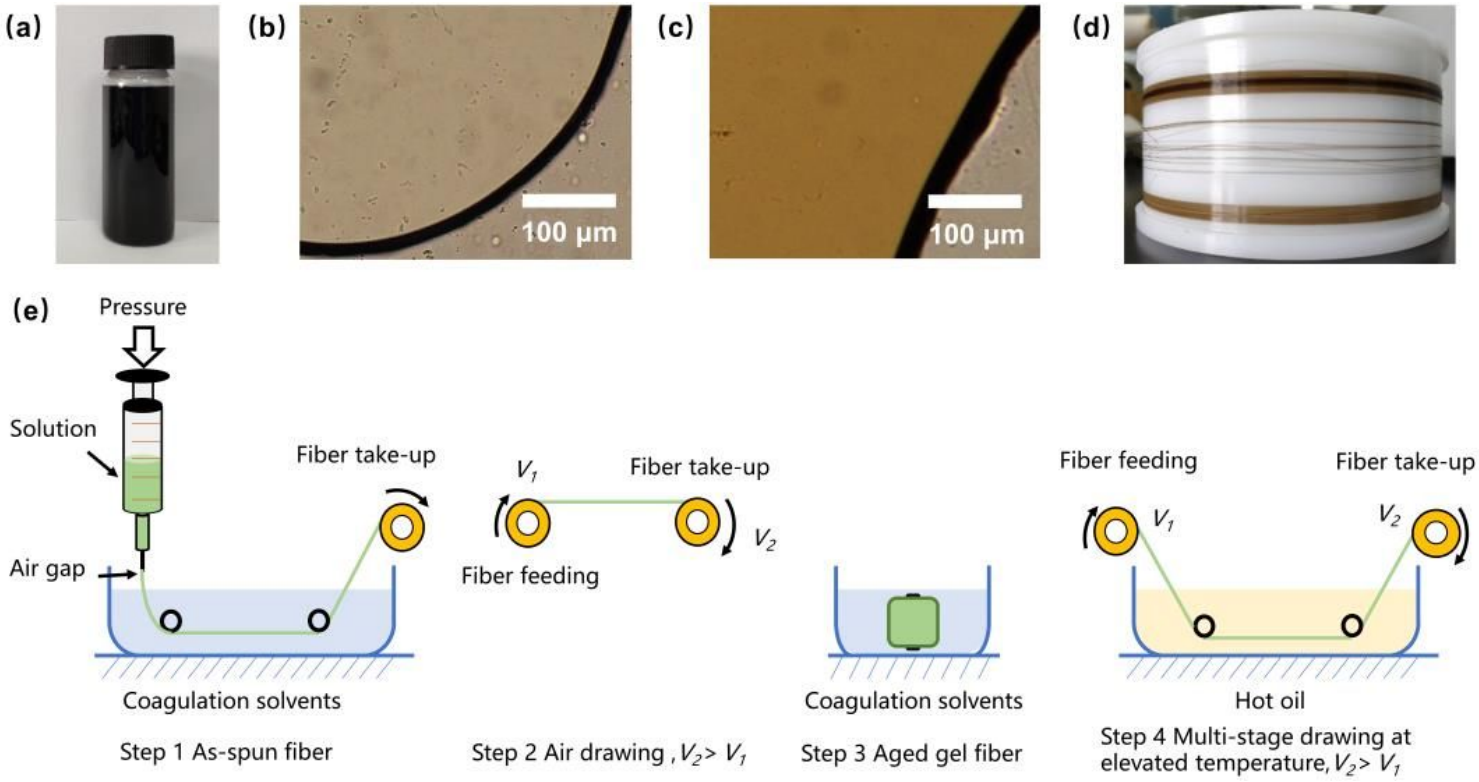

Figure 1

Homogeneity of GO/lignin/PVA dopes: (a) digital photograph of 0.2% GO/30% lignin/PVA solution, and optical micrographs of (b) 0.2% GO/5% lignin/PVA and (c) 0.2% GO/30% lignin/PVA spinning solutions; (d) digital photograph of 30% lignin/PVA drawn fibers prepared by gel spinning, (e) the fiber gel spinning process: as-spun gel fiber formation (Step 1), air drawing (Step 2), gel fiber aging (Step 3), and multiple-stage fiber drawing (Step 4)

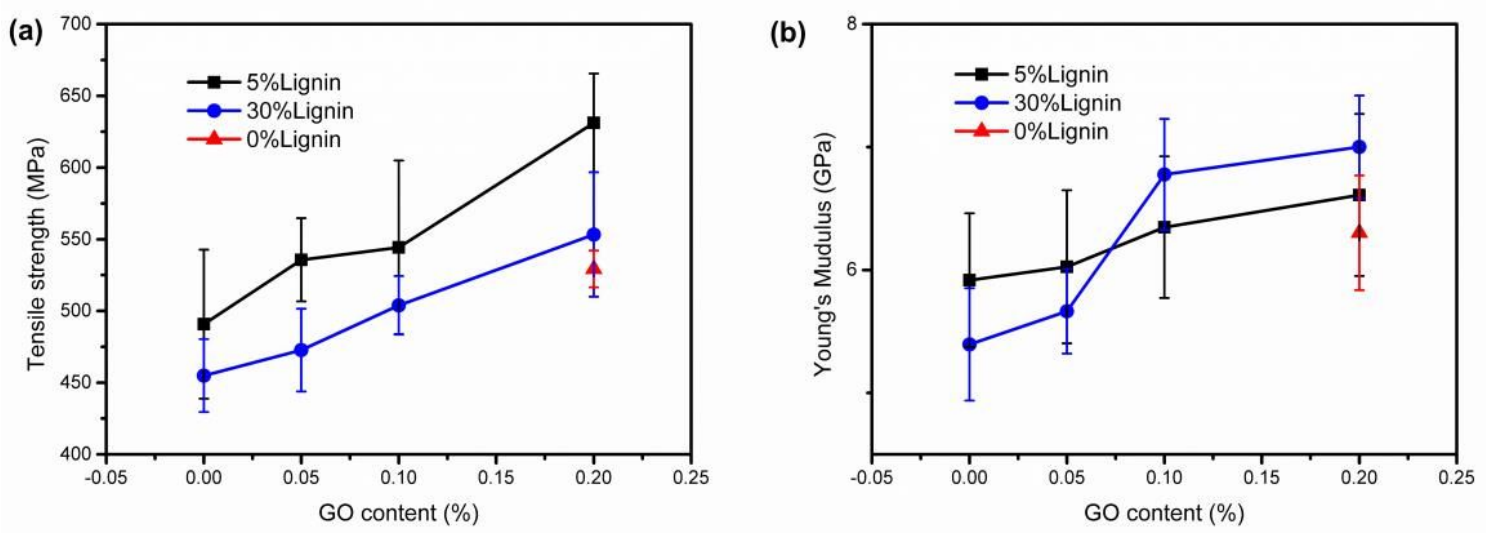

Figure 2

Tensile strength and Young’s modulus of gel-spun PVA fibers of 0/5/30% lignin and 0/0.05%/0.1%/0.2% GO

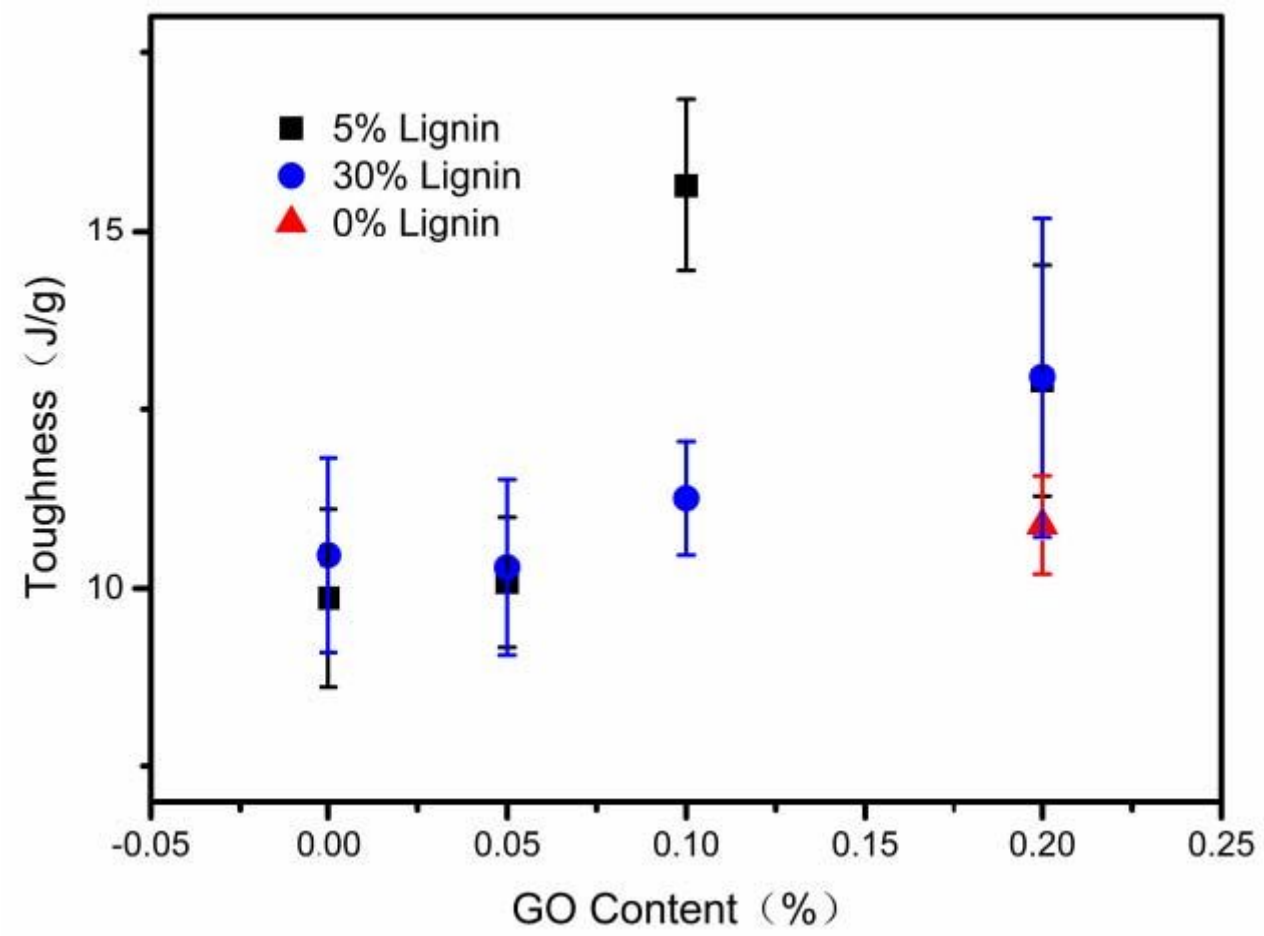

Figure 3

Toughness of gel-spun PVA fibers with 0/5/30% lignin and 0/0.05%/0.1%/0.2% GO

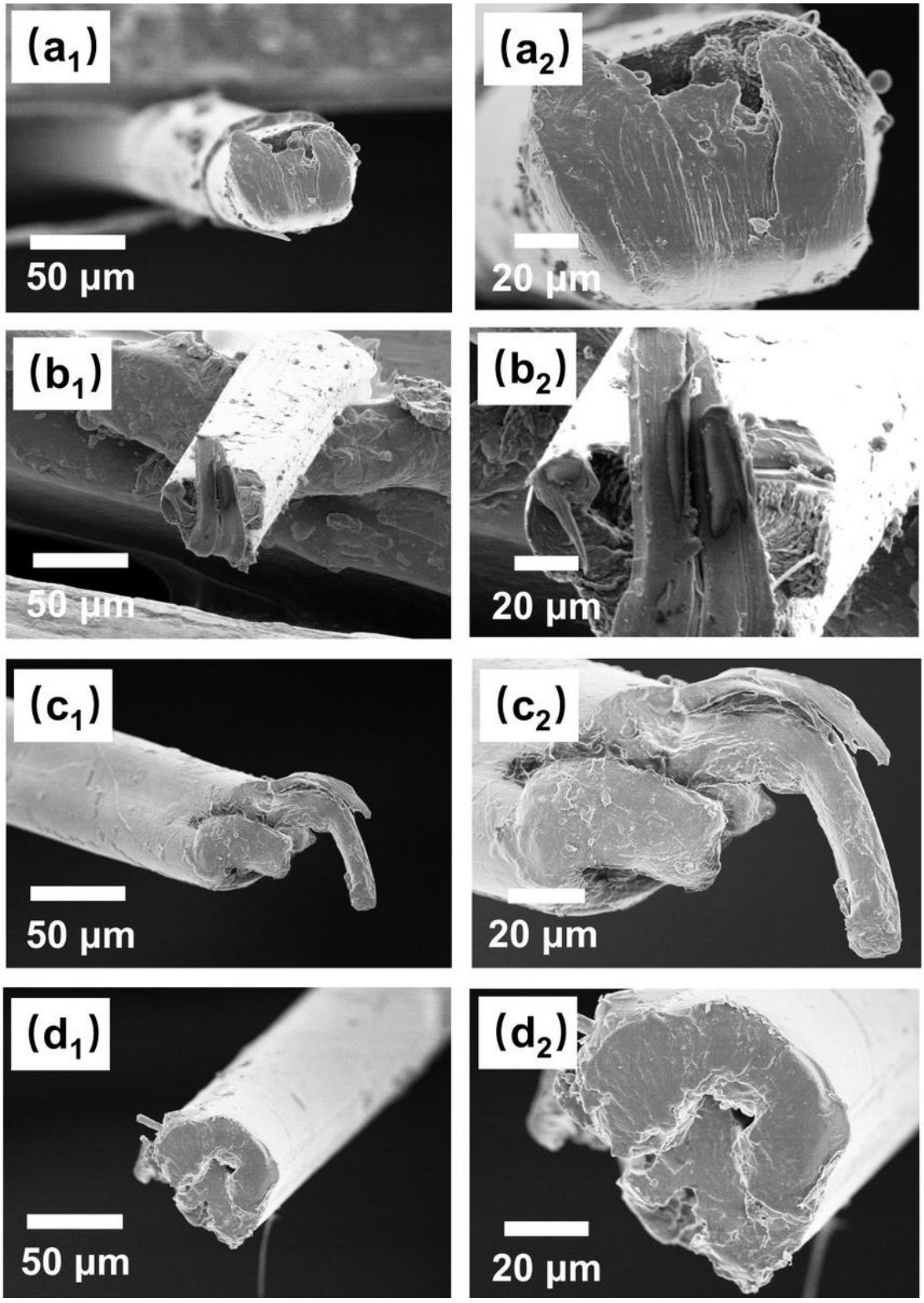

Figure 4

(1) Low- and (2) high-resolution SEM images of fracture tips of (a) 5% lignin /PVA fibers, (b) 0.2% GO/5% lignin/PVA fibers, (c) 30% lignin/PVA fibers, (d) 0.2% GO/30% lignin/PVA fibers

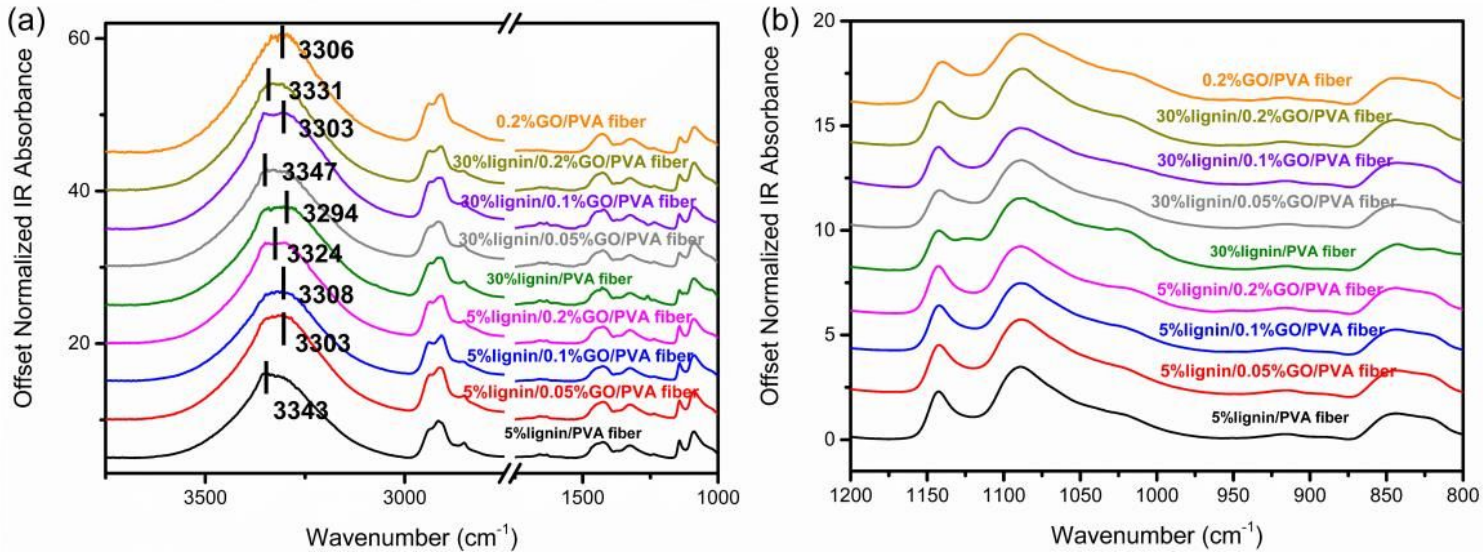

Figure 5

FTIR absorbance spectra of gel-spun composite fibers between (a) 4200–1000 cm-1 and (b) 1250–800 cm-1

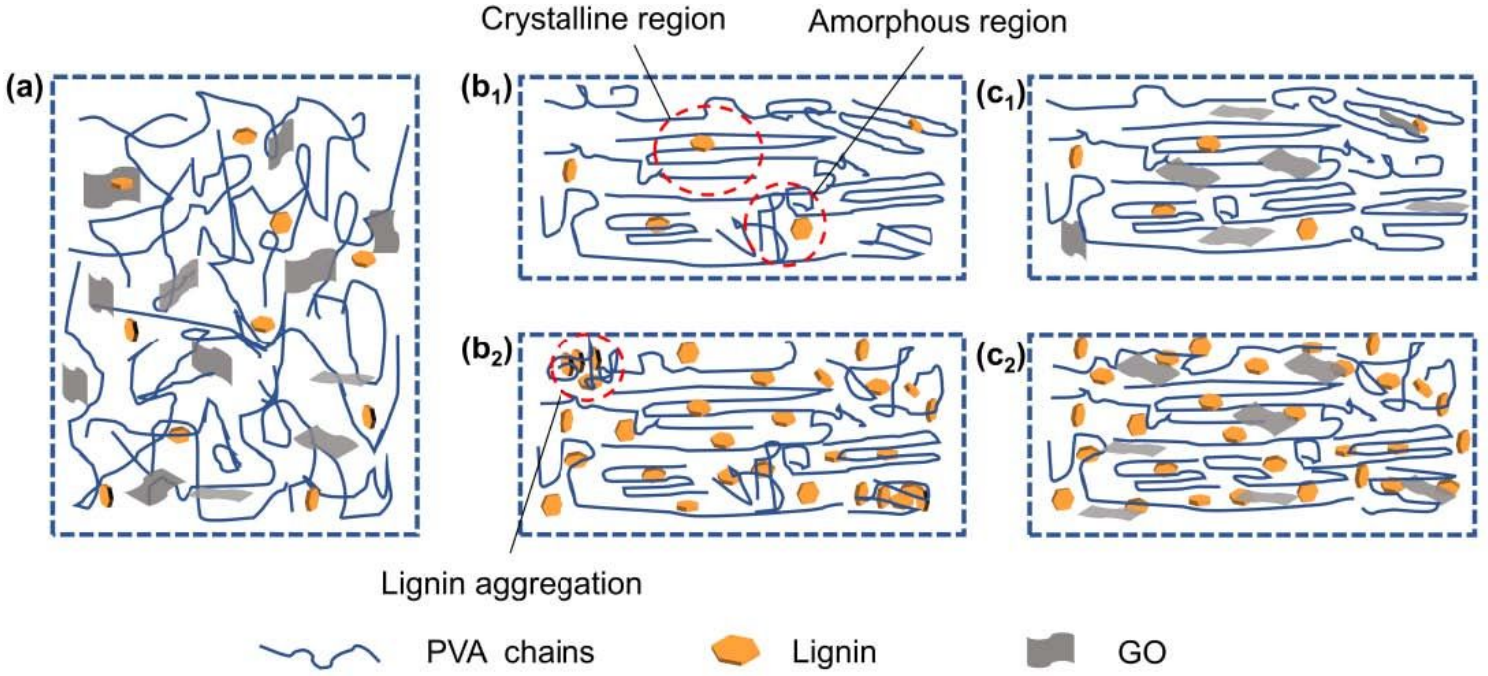

Figure 6

The microstructure model of (a) GO/lignin/PVA spinning dope and (1) 5% (2) 30% lignin/PVA fibers (b) without and (c) with GO

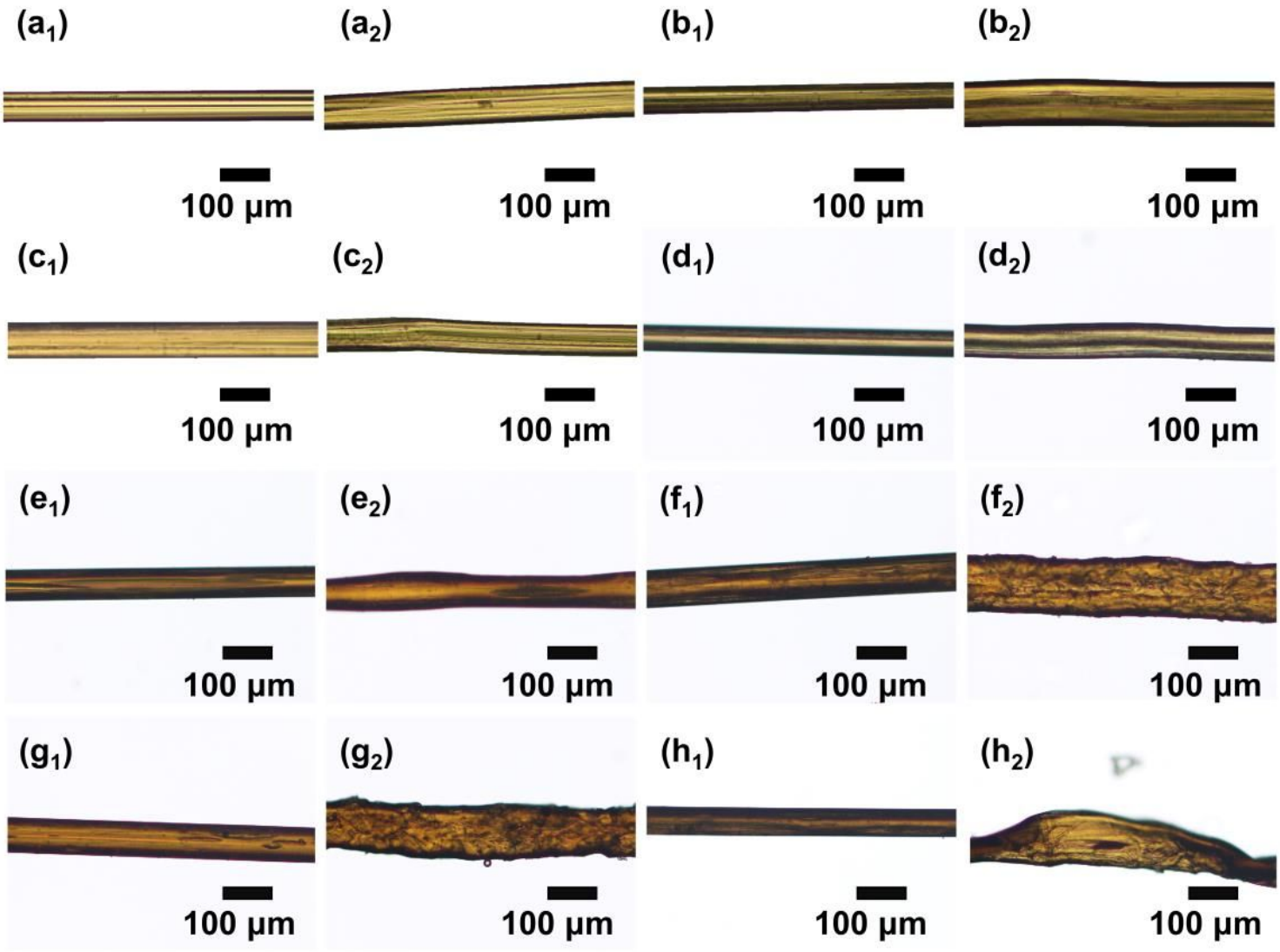

Figure 7

Optical micrographs of (a) 5% lignin/PVA fiber, (b) 0.05% GO/5% lignin/PVA fiber, (c) 0.1% GO/5% lignin/PVA fiber, (d) 0.2% GO/5% lignin/PVA fiber, (e) 30% lignin/PVA fiber, (f) 0.05% GO/30% lignin/PVA fiber, (g) 0.1% GO/30% lignin/PVA fiber, (h) 0.2% GO/30% lignin/PVA fiber after water immersion at (1) 25 °C and (2) 85 °C

Supplementary Files

This is a list of supplementary files associated with this preprint. Click to download.

- SupplementaryInformation.docx
- GraphicalAbstract.jpg